Amino Acids (2015) 47:2293–2302
DOI 10.1007/s00726-015-2008-z

ORIGINAL ARTICLE

Optically active poly(amide–imide)/TiO_2 nanocomposites containing amino acid moieties: synthesis and properties

Zahra Rafiee[1] · **Elham Zare**[1]

Received: 12 January 2015 / Accepted: 11 May 2015 / Published online: 23 May 2015

Abstract The novel optically active poly(amide–imide) (PAI)/TiO_2 nanocomposites containing fluorene moieties have been successfully synthesized through ultrasonic irradiation. The surface of nanoparticles was chemically modified with γ-aminopropyltriethoxyl silane to enhance the compatibility with polymeric matrix and to avoid the aggregation of nanoparticles. The dispersion of surface-modified TiO_2 in PAI film was confirmed by the transmission electron microscope (TEM) analysis showing the well-dispersed nanosized TiO_2 nanoparticles. The thermal stabilities and optical properties of PAI/surface-modified TiO_2 nanocomposite films were also investigated. The thermogravimetric analysis data showed an improvement of thermal stability of novel nanocomposite films as compared to the pure polymer.

Keywords Poly(amide–imide) · Nanocomposite · Amine-functionalized TiO_2 · TiO_2

Introduction

Polymer nanocomposites have attracted intense research interest owing to their unique physical and chemical properties resulting from the combination of organic and inorganic materials in single compound. They possess optical, electronic, magnetic properties, and exceptional applications in high-technological fields (Hu et al. 2014; Lim et al. 2013; Liu et al. 2015; Mallya et al. 2014; Rafiee and Golriz 2015). Nanotitaniae (n-TiO_2) has been widely studied because of high physical and chemical stability, nontoxicity, relatively low price and easy availability. They have been widely applied in pigments (El-Sherbiny et al. 2014), photocatalysts (Schneider et al. 2014), catalyst supports (Derlyukova et al. 2012), solar cell (Frank et al. 2004), gas sensors (Haidry et al. 2011), and so on.

Aromatic polyamides (PA)s are hydrophilic polymers that can absorb water due to their amide units (Ayala et al. 2005). Hence, these polymers are good candidates for semipermeable membranes, particularly for the filtration of aqueous solutions and for water purification (Wang et al. 2011). However, aromatic PAs are difficult to process because of their high glass transition temperatures and poor solubility in organic solvents. The incorporation of bulky pendent groups produces a chain separation effect lowering the chain packing, which increases water accessibility and improves solubility (Mallakpour and Rafiee 2011). Poly(amide–imide)s (PAI)s are a kind of thermoplastic resin, have good high-temperature resistance, excellent mechanical strength and high oxidative stability, all of which have led PAI to have been widely applied with electronic materials, adhesives, composite materials, fiber, and film material (Hamciuc et al. 2015; Mallakpour and Rafiee 2011; Mallakpour et al. 2014). Comparing with the polyimides and PAs, the PAIs offer the better process ability and heat-resistant properties. The PAIs have attracted increasing interest for a wire-coating material with a thermal resistant property.

The combination of amino acid residues into synthetic polymers is of attention since these combinations produce new non-biological macromolecules with biomimetic structures and properties and hence have many potential

Handling Editor: H. S. Sharma.

✉ Zahra Rafiee
zahrarafiee2004@yahoo.com; z.rafiee@mail.yu.ac.ir

[1] Department of Chemistry, Yasouj University, 75914-74831 Yasouj, Islamic Republic of Iran

applications, including optical resolution, controlled drug release systems, and biologically active and degradable materials (Baughman and Wagener 2005; Katsarava 2003; Sanda and Endo 1999). Among the synthetic PAs, only those containing the naturally occurring (L)-α-amino acids, being structurally close to the natural polypeptides, possess potentially degradable linkages that make them suitable as biomaterials (Niaounakis 2013).

In this study, chiral and thermally stable PAI containing pendant fluorene groups based on a synthesized diamine, 3,5-diamino-*N*-(9H-fluoren-2-yl)benzamide and diacid chloride, *N,N′*-(pyromellitoyl)-bis-S-valine diacid chloride was prepared. Then, we propose a simple ultrasonication-assisted solution blending process for fabricating nanocomposites and a casting technique for the preparation of nanocomposite films.

Experimental

Materials

All chemicals were purchased from Fluka Chemical (Buchs, Switzerland), Aldrich Chemical (Milwaukee, WI), RiedeldeHaen (Seelze, Germany) and Merck Chemical. Pyromellitic dianhydride (benzene-1,2,4,5-tetracarboxylic dianhydride) (from Merck) was purified with acetic anhydride in boiling acetic acid. *N,N′*-dimethylacetamide (DMAc) was dried over BaO, and then distilled in vacuum. S-Valine and triethylamine (TEA) were purchased from Merck and used as obtained without further purification. TiO_2 nanoparticles were purchased from Neutrino Co. The silane coupling agent (γ-aminopropyltriethoxyl silane) (APTES, KH550) was purchased from Merck Chemical Co.

Techniques

Proton nuclear magnetic resonance (^{1}H-NMR, 400 MHz) spectra were recorded on a Bruker (Germany) Avance 400 instrument in dimethyl sulfoxide (DMSO)-d_6 solution. FT-IR spectra were recorded on (Jasco-680, Japan) spectrophotometer. Inherent viscosities were measured using a Cannon–Fenske Routine Viscometer (Germany) at concentration of 0.5 g dL^{-1} in DMF at 25 °C. UV–Vis spectra were recorded on a UV/Vis/NIR spectrophotometer, JASCO, V-570. TGA data for polymers were taken on STA503 WinTA instrument at a heating rate of 20 °C min^{-1} under nitrogen atmosphere. The XRD patterns were recorded by employing a Philips X'PERT MPD diffractometer Cu Kα radiation: λ = 0.154056 nm at 40 kV and 30 mA over the 2θ range of 10–80° at a scan rate of 0.05°/min. The morphology and dispersity analysis were performed on transmission electron micrograph (TEM) analyzer on Philips CM 120 operating at 100 kV. The reaction was carried out on a Misonix ultrasonic liquid processor, XL-2000 Series. Ultrasound was a wave of frequency 2.25×10^4 Hz and power 100 W.

Monomers synthesis

Synthesis of N-(9H-fluoren-2-yl)-3,5-dinitrobenzamide (3)

Into a 25-mL round-bottomed flask fitted with a magnetic stirrer, a solution of 0.200 g (1.10×10^{-3} mol) 2-aminofluorene (1) in 3 mL of dry NMP was placed. The reaction mixture was cooled in an ice water bath. To this mixture 0.254 g (1.10×10^{-3} mol) of 3,5-dinitrobenzoyl chloride, (2) in 2 mL of NMP was added dropwise. The mixture was stirred in ice bath for 3 h, and then 0.75 mL of triethylamine was added. The mixture was stirred in ice bath for 2 h and at room temperature overnight. The resulting mixture was poured into 10/30 mL of cold water/concentrated HCl. The precipitate was collected by filtration and washed thoroughly with water and dried at 70 °C for 8 h to yield 0.39 g (95 %) of compound 3. Recrystallization from DMF/water gave orange crystals. mp 309 °C. FT-IR (KBr, cm^{-1}): 3262 (N–H stretch), 1651 (C=O stretch), 1538, 1341 (–NO_2 stretch). ^{1}H NMR (DMSO-d_6, ppm): 10.94 (s, 1H, N–H), 9.21 (d, 2H, Ar, J = 7.2 Hz), 9.01 (t, 1H, Ar, J = 2.1 Hz), 8.13 (d, 1H, Ar, J = 0.8 Hz), 7.93 (d, 1H, Ar, J = 8.3 Hz), 7.87 (d, 1H, Ar, J = 7.5 Hz), 7.79 (dd, 1H, Ar, J = 1.8 Hz, J = 8.3 Hz), 7.59 (d, 1H, Ar, J = 7.4 Hz), 7.40 (t, 1H, Ar, J = 7.2 Hz), 7.31 (dt, 1H, Ar, J = 1.0 Hz, J = 7.4 Hz), 3.98 (s, 2H, CH_2).

Synthesis of 3,5-diamino-N-(9H-fluoren-2-yl)benzamide (4)

0.200 g (5.33×10^{-4} mol) of the dinitro compound 3, 0.01 g of 10 % Pd/C, and 10 mL of ethanol were introduced into a two-necked flask. The suspension solution was heated to reflux, and 3 mL of hydrazine monohydrate was added dropwise. After the complete addition, the reaction was continued at reflex temperature for another 12 h. To the suspension, 10 mL of THF was added to redissolve the precipitated product, and refluxing was continued for 90 min. The mixture was filtered to remove the Pd/C and the filtrate was distilled to remove the solvent. The crude product recrystallized from ethanol and dried in vacuo at 80 °C to give 0.14 g (yield 86 %) of compound 4. mp 255 °C. FT-IR (KBr, cm^{-1}): 3466, 3439, 3360 and 3330 (N–H stretch), 1650 (C=O stretch). ^{1}H NMR (DMSO-d_6, ppm): 10.03 (s, 1H, N–H), 8.09 (d, 2H, Ar, J = 1.1 Hz), 7.83 (d, 2H, Ar, J = 8.3 Hz), 7.71 (dd, 1H, Ar, ^1J = 1.9 Hz, ^2J = 8.3), 7.56 (d, 1H, Ar, J = 1.9 Hz), 7.36 (t, 1H, Ar, J = 6.8 Hz), 7.27 (dt, 1H, Ar, ^1J = 1.1 Hz, ^2J = 7.4 Hz), 6.31 (d, 2H,

Ar, $J = 1.9$ Hz), 6.01 (t, 1H, Ar, $J = 1.9$ Hz), 4.96 (s, 4H, $2NH_2$), 3.91 (s, 2H, CH_2).

N,N′-(pyromellitoyl)-bis-S-valine diacid (7)

Into a 50-mL round-bottomed flask, 1.0 g (4.58 mmol) of pyromellitic dianhydride (5), 1.07 g (9.16 mmol) of s-valine (6), 15.0 mL of acetic acid and a stirring bar were placed. The mixture was stirred at room temperature for 5 h and then was refluxed for 6 h. The solvent was removed under reduced pressure and 25 mL of cold HCl 10 % was added to the residue and stirred for 1 h. A white precipitate was formed, filtered off, washed with water and dried under vacuum at 80 °C to give 1.75 g (92 %) of compound (7). Recrystallization from methanol/water gave white crystals. mp: 265-267 °C, $R_f = 0.85$ (60:40; ethylacetate:cyclohexane), $[\alpha]_D^{25} = -116.0$ [0.050 g in 10 mL *N,N′*-dimethylformamide (DMF)]. IR (KBr, cm^{-1}): 2400–3500 (s, br), 1760 (s, sh), 1720 (s, br), 1460 (m), 1440 (m), 1380 (s), 1360 (s), 1260 (s), 1150 (m), 1080 (s), 1020 (m), 890 (s), 820 (m), 780 (m), 720 (s), 620 (m). ^{1}H NMR (DMSO-d_6, ppm): 11.3 (a broad peak for two acidic –OH protons), 8.5 (s, 2H), 4.5 (d, 2H), 2.5–2.9 (m, 2H), 0.8–1.3 (dd, 12H). Found: C, 57.68 %; H, 4.92 %; N, 6.95 % ($C_{20}H_{20}N_2O_8$ requires C, 57.69 %; H, 4.84 %; N, 6.73 %).

N,N′-(pyromellitoyl)-bis-S-valine diacid chloride (8)

Into a 25-mL round-bottomed flask, 0.50 g (1.20 mmol) of compound 7 and 4.0 mL (an excess amount) of thionyl chloride were placed. The mixture was stirred at room temperature for 2 h and then was refluxed for 1 h. Unreacted thionyl chloride was removed under reduced pressure and the residue was washed with *n*-hexane, to leave 0.53 g (98.0 %) of diacid chloride (5). mp: 138-140 °C, $[\alpha]_D^{25} = -137.2$ (0.050 g in 10 mL DMF). IR (KBr, cm^{-1}): 3100 (w), 2950 (s), 2900 (m), 1820 (s, sh), 1790 (s), 1720 (s, br), 1460 (s), 1380 (s), 1360 (s), 1340 (s), 1270 (m), 1250 (w), 1150 (s), 1120 (m), 1080 (s), 1050 (s), 1020 (m), 990 (m), 910 (s), 860 (m), 840 (m), 810 (m), 770 (s), 730 (s), 620 (s), 580 (w).

Synthesis of PAI

An optically active PAI was synthesized by four different methods:

Method I To a 25-mL round-bottomed flask equipped with a nitrogen inlet and a water-cooled condenser, 0.10 g (2.21×10^{-4} mol) of diacid chloride 8, 0.069 g (2.21×10^{-4} mol) of diamine 4 and 1 mL of DMAc were added. The reaction system was heated to reflux at 100 °C affording a viscous polymer solution. The resulting viscous solution was precipitated into 30 mL of methanol, filtered and dried under vacuum to give 0.127 g (75 %) of PAI-I. The inherent viscosity (η_{inh}) of the polymer in DMF was 0.31 dL g^{-1}, measured at a concentration 0.5 g dL^{-1} at 25 °C. $[\alpha]_D^{25} = -63.7$ (0.050 g in 10 mL DMF).

Method II Into a 25-mL round-bottomed flask fitted with a magnetic stirrer, a solution of 0.10 g (2.21×10^{-4} mol) of diacid chloride 8, 0.069 g (2.21×10^{-4} mol) of diamine 4 and 1 mL of DMAc was placed. The reaction mixture was stirred for 30 min under a nitrogen atmosphere at room temperature. Then 0.31 mL (2.21×10^{-4} mol) of TEA was added. The resulting mixture was stirred for 7 h at room temperature. The solution became viscous as the polymer formed. The resulting viscous solution was precipitated into 30 mL of methanol, filtered and dried under vacuum to give 0.142 g (84 %) of PAI-II. $\eta_{inh} = 0.57$ dL g^{-1}. $[\alpha]_D^{25} = -98.3$ (0.050 g in 10 mL DMF).

Method III A mixture of 0.10 g (2.40×10^{-4} mol) of diacid 7, 0.076 g (2.40×10^{-4} mol) of diamine 4, 0.06 g of calcium chloride, 0.30 g (9.61×10^{-4} mol) of TPP, 0.15 mL of Py and 0.5 mL of NMP was refluxed for 3 h. After cooling, the reaction mixture was poured into 30 mL of methanol with constant stirring, and the precipitate was washed thoroughly with methanol and hot water, collected on a filter, and dried under vacuum to give 0.144 g (82 %) of PAI-III. $\eta_{inh} = 0.22$ dL g^{-1}. $[\alpha]_D^{25} = -61.2$ (0.050 g in 10 mL DMF).

Method IV Into a 25-mL round-bottomed flask in an ice bath, 0.10 g (2.21×10^{-4} mol) of diacid chloride 8, 3 mL of dichloromethane and a stirring bar were placed. A solution of 0.069 g (2.21×10^{-4} mol) of diamine 4 in water (2.5 mL), sodium hydroxide (1.5 mL, 0.1 N) and catalytic amount of tetraethylammonium bromide was prepared. This solution was added dropwise to the flask during 10 min with stirring the mixture vigorously. After stirring for 3 h, the polymer was filtered off, washed with methanol, and vacuum dried at 90 °C to give 0.101 g (60 %) of PAI-IV. $\eta_{inh} = 0.41$ dL g^{-1}. $[\alpha]_D^{25} = -56.3$ (0.050 g in 10 mL DMF).

Surface functionalization of nano-TiO_2 with APTES

Nano TiO_2 was dried at 110 °C in an oven for 24 h to remove the adsorbed water. The dried nano TiO_2 (0.2 g) was ultrasonicated for 15 min in 10 mL of absolute ethanol and then 0.042 mL of APTES (20 wt% TiO_2) was added to the dispersed solution; then, the mixture was dispersed for 1 h through an ultrasonic bath. Finally, the suspension was filtrated and washed with ethanol to remove unreacted APTES. The solid was dried at 60 °C for more than 24 h.

Preparation of PAI/TiO_2 nanocomposites

0.1 g of PAI-II was dispersed in 20 mL of absolute ethanol. A uniform colloidal dispersion was obtained after

Scheme 1 Synthesis of diamine 4

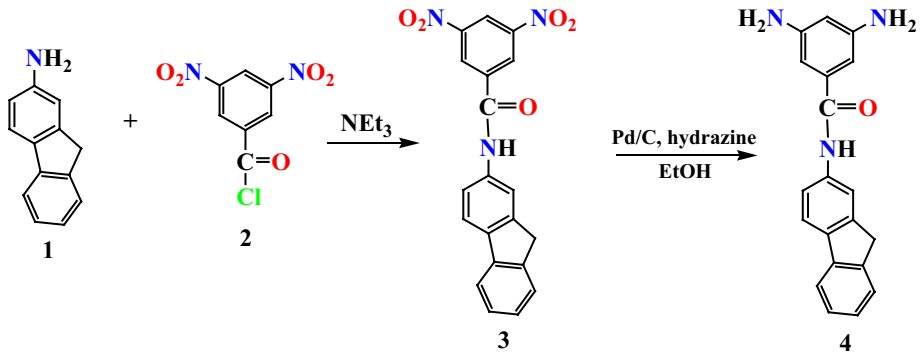

ultrasonication for about 20 min through an ultrasonic bath. Then different amounts of modified TiO_2 nanoparticles (2, 4, 6, 8 and 10 % W/W based on the PAI content) were added to the resulting suspension and the mixture was ultrasonicated for 4 h. After irradiation, the solvent was removed, and obtained nanocomposites were dried in vacuum at 80 °C for 6 h.

Pure PAI: FT-IR (KBr): υ = 3420 (s), 2968 (m), 1774 (m), 1723 (s), 1600 (m), 1541 (m), 1456 (s), 1383 (s), 1353 (m), 1227 (m), 767 (m), 730 (m) cm^{-1}.

PAI/TiO_2 10 wt%: FT-IR (KBr): υ = 3411 (s), 2965 (m), 1774 (m), 1718 (s), 1600 (m), 1540 (m), 1382 (m), 1352 (m), 1078 (m), 767 (m), 730 (m), 565 (m, br) cm^{-1}.

Results and discussion

Synthesis of monomers

The synthetic route of the diamine monomer, 3,5-diamino-*N*-(9H-fluoren-2-yl)benzamide (4) is outlined in Scheme 1 (Rafiee and Golriz 2014). *N*-(9H-Fluoren-2-yl)-3,5-dinitrobenzamide (3) was prepared by the condensation of 2-aminofluorene (1) and 3,5-dinitrobenzoyl chloride (2). The new aromatic diamine having a bulky pendent fluorenamide group, 3,5-diamino-*N*-(9H-fluoren-2-yl)benzamide (4), was successfully synthesized by hydrazine Pd/C-catalytic reduction according to the synthetic route outlined in Scheme 1. The purity of monomer 4 was checked by thin-layer chromatography, which showed one spot in an ethyl-acetate/cyclohexane mixture (50:50) with R_f = 0.38. FT-IR and ^{1}H NMR spectroscopic techniques were applied to identify the structures of the compound 3 and the diamine monomer 4. The transformation of nitro to amino functionality could be monitored by the change of FT-IR spectra. The nitro groups of compound 3 gave two characteristic bands at around 1538 and 1341 cm^{-1} ($-NO_2$ asymmetric and symmetric stretching). After reduction, the characteristic absorptions of the nitro group disappeared and the amino group showed the typical N–H stretching absorption pair in the region of 3466-3330 cm^{-1}. The ^{1}H NMR spectra of compound 3 and the diamine monomer 4 agree well with the proposed molecular structure of compounds 3 and 4. The ^{1}H NMR spectrum confirms that the nitro groups have been completely transformed into amino groups by the high field shift of the aromatic protons and by the resonance signals at 4.96 ppm corresponding to the amino protons.

N,N′-(Pyromellitoyl)-bis-S-valine diacid chloride (8) was prepared by the three-step procedure as shown in Scheme 2 (Mallakpour and Shahmohammadi 2005). The symmetric diacid compound 7 was synthesized by the condensation reaction of pyromellitic dianhydride (5) with two moles of S-valine (6) in acetic acid. The intermediate amic-acid was not isolated, and dehydration was performed under refluxing condition. The resulting symmetric diacid 7 was converted to its diacid chloride derivative 8 by reaction with thionyl chloride. The monomer 8 was purified by washing with *n*-hexane to remove thionyl chloride. Chemical structure and purity of the optically active monomers 7 and 8 were proved using elemental analysis, IR and ^{1}H NMR spectroscopic techniques. The broad peak at 11.3 ppm in the ^{1}H NMR is assigned to the carboxylic acid protons and the absorption of aromatic protons has been appeared as a singlet at 8.5 ppm. The protons of the chiral center, which appeared as a doublet at 4.5 ppm have the coupling constant of 6.0 Hz. Absorption of the proton appears as a multiplet from 2.5 to 2.9 ppm. The peaks of methyl protons have been appeared as a doublet of doublet at a range of 0.8–1.3 ppm which is due to diastereotopic methyl protons.

The IR spectrum of compound 7 showed a broad and strong peak at 2400–3500 cm^{-1} which was assigned to the COOH groups and two absorption bands at 1720 and 1760 cm^{-1} are characteristic peaks of carbonyl groups of imide rings. Disappearance of strong acidic hydroxyl peak in IR spectrum of compound 8 confirmed a complete conversion of diacid 7 to diacid chloride 8. On the other hand, because of the electron-withdrawing character of the Cl

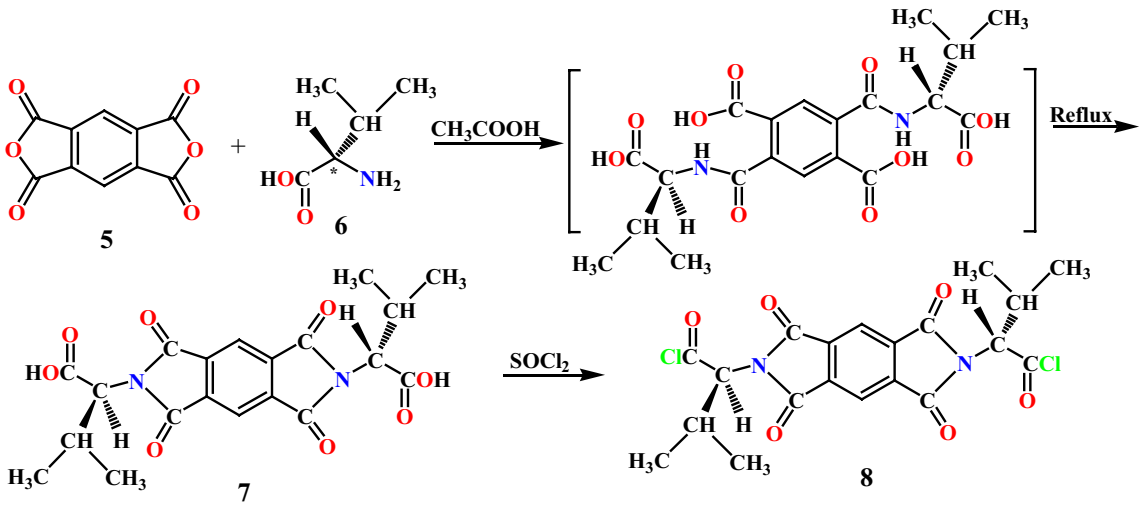

Scheme 2 Synthesis of diacid chloride 8

groups, the two carbonyl peaks of diacid chloride in comparison with its starting diacid were shifted to higher frequency. The reaction was completed after 3 h. The resulting monomers showed optical rotations, which indicated that they are optically active. Then, they were used for the synthesis of optically active polymers.

Polymer synthesis

The polymerization of aromatic diamine, 3,5-diamino-*N*-(9H-fluoren-2-yl)benzamide (4) with diacid 7 or diacid chloride 8 was performed using four different methods to produce an optically active PAI. In method I, the polycondensation reaction was performed in DMAc solution in 100 °C. In method II, the polycondensation reaction was performed in DMAc solution in room temperature in the presence of TEA. In method III, PAI was synthesized by Yamazaki–Higashi phosphorylation polyamidation technique of diamine 4 with chiral dicarboxylic acid 7. In method IV, interfacial polymerization was applied to prepare the PAI in the presence of catalytic amount of tetraethylammonium bromide. The highest yield and inherent viscosity of PAI were obtained from method II.

The structure of the PAI was confirmed by FT-IR and ^{1}H NMR spectroscopic analyses. The FT-IR spectrum of this polymer showed absorptions around 3420 cm^{-1} (N–H), 1774 cm^{-1} (C=O asymmetric, imide), 1723 cm^{-1} (C=O symmetric, imide), 1600 cm^{-1} (C=O, amide). The presence of the imide heterocycle in this polymer was revealed by absorption of 1383 and 730 cm^{-1} which belong to carbonyl bendings of imide. Figure 1 shows the high-resolution ^{1}H NMR spectrum of PAI. The assignments of the ^{1}H NMR spectra agree well with the proposed polymer structure (Scheme 3).

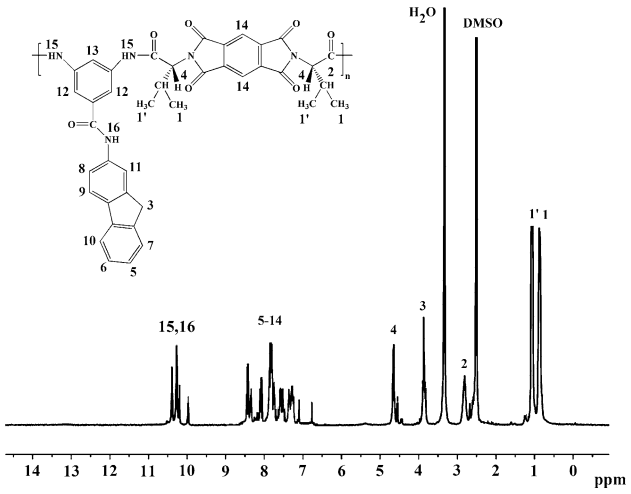

Fig. 1 ^{1}H NMR spectrum of PAI in DMSO-d_6 solution

Surface modification of TiO_2 nanoparticles

Surface-treating TiO_2 filler with a suitable modifying agent can improve the compatibility of TiO_2 filler with polymeric matrix, promotes effectively the adhesion of polymeric matrix to TiO_2 filler, and reduces the aggregation of nanoparticles in polymer/TiO_2 nanocomposite. In this investigation, the surface of TiO_2 nanoparticles was treated via APTES. Hydroxyl groups that exist on the surface of TiO_2 nanoparticles can replace with OCH_2CH_3 of the APTES to bond to it. In this way, the surface of TiO_2 was changed to hydrophobic that can have good affinity to organic matrix. As a result, the modified TiO_2 nanoparticles can fulfill steric hindrance between inorganic nanoparticles and organic polymer to obtain uniform dispersion and prevent the aggregation process. For coupling agent APTES,

Scheme 3 Synthesis of PAI

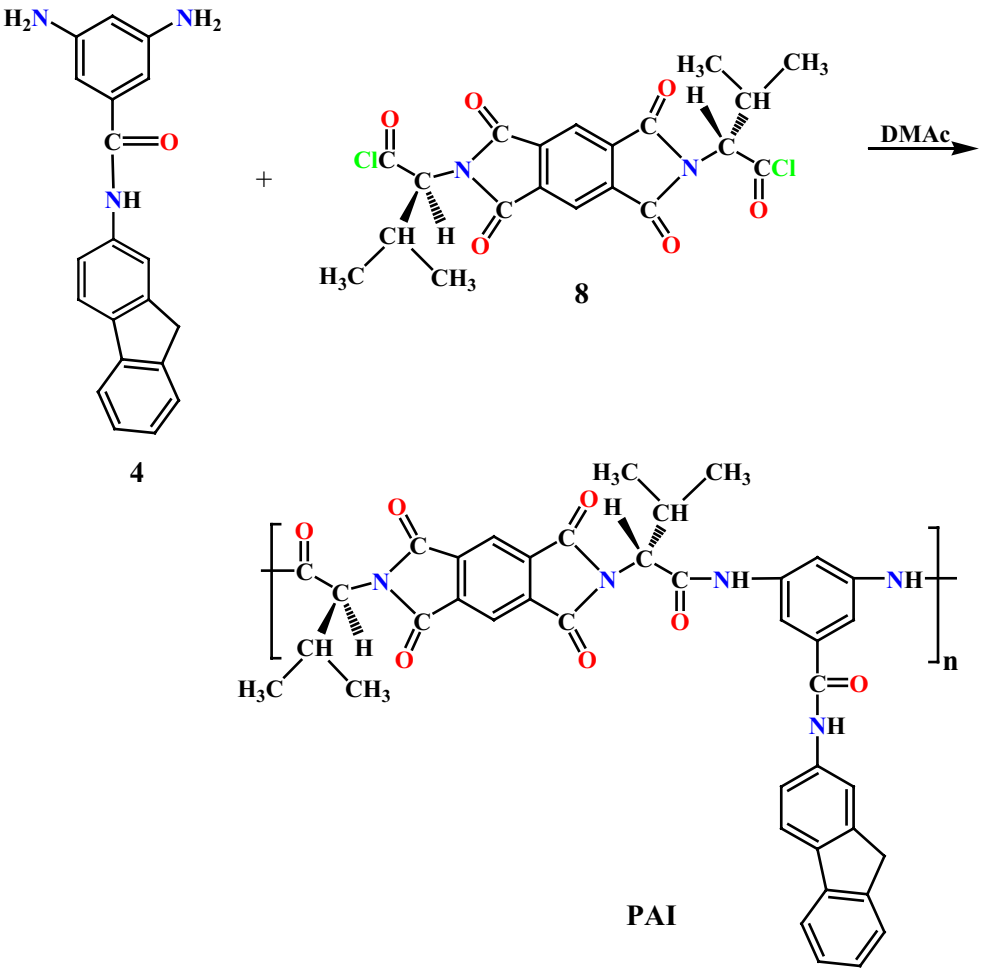

the functional group that provides different interactions to TiO_2 nanoparticle is the amino group. Various interaction types between aminosilane and TiO_2 surface were proposed as follows: (a) hydrogen bonding (b) ionic bonding and (c) covalent bonding with surface hydroxyl groups. The details of the mechanism are shown in Scheme 4. FT-IR spectra of as-received TiO_2 nanoparticles and APTES-modified TiO_2 nanoparticles are shown in Fig. 2 together with the spectrum of pure APTES molecule.

For pure TiO_2 nanoparticles, the broad absorption band at 3400 cm^{-1} is assignable to stretching motions of the surface hydroxyl or the adsorption water and the peak at 1630 cm^{-1} corresponds to vibration of O–H bonds on the TiO_2 nanoparticles surface. The broad absorption band observed in the region 450–800 cm^{-1} corresponds to Ti–O stretching. Furthermore, new bands appeared at 2870–2928 cm^{-1} in the FT-IR spectrum of modified TiO_2 nanoparticles, which are attributed to C–H stretching band of γ-aminopropyl groups of APTES. From the spectral data, it can be deduced that the APTES has been grafted on TiO_2 nanoparticles to produce an organic layer connecting with TiO_2 nanoparticles.

Nanocomposites synthesis

PAI/TiO_2 nanocomposites containing fluorene and S-valine moieties were prepared by an ultrasonic irradiation technique. Different amounts of modified TiO_2 nanoparticles were mixed with the PAI and the mixture was dispersed in DMAc under ultrasonic irradiation. When modified nanoparticles are embedded into PAI matrix, hydrogen bonding between PAI and modified nanoparticles was formed. Consequently, the dispersity of nanoparticles could be greatly improved.

The FT-IR spectra of PAI and PAI/TiO_2 nanocomposites with different contents of TiO_2 nanoparticles are shown in Fig. 3. FT-IR spectrum of PAI showed the characteristic absorptions of amide and imide groups occurring around, 3420, 1774, 1723 and 1600 cm^{-1}, which are peculiar to N–H stretching, C=O stretching of imide and amide, respectively. Compared with pure PAI, a new broad absorption band around 450–800 cm^{-1} can be found in the spectra of PAI/TiO_2 nanocomposites, which increases with TiO_2 percent and can be attributed to the vibration of Ti–O–Ti groups.

XRD patterns of PAI (a), pure TiO_2 nanoparticles (b) and PAI/TiO_2 nanocomposite 8 wt% (c) are given in Fig. 4.

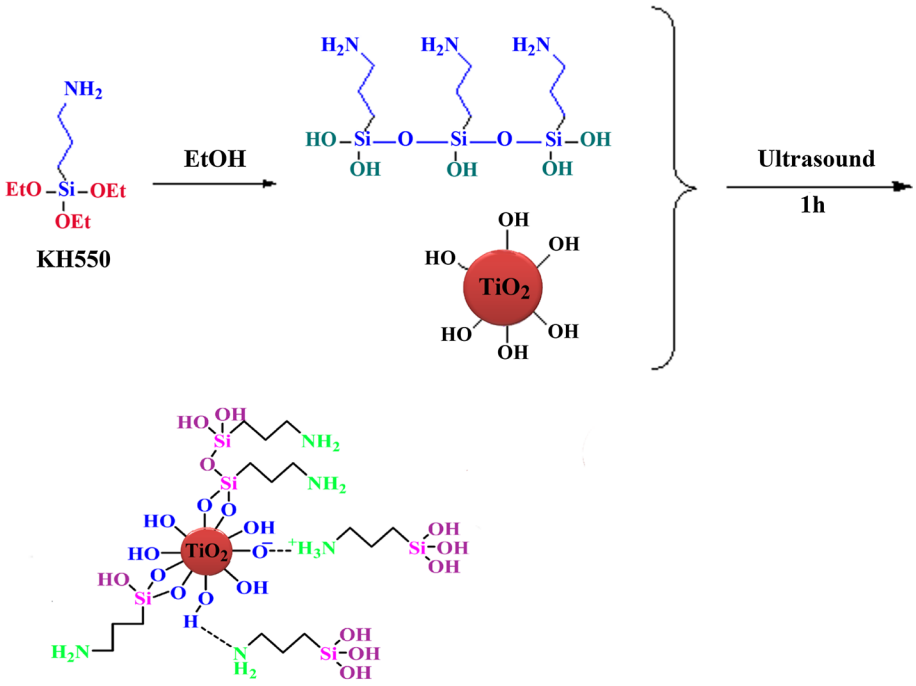

Scheme 4 Surface modification of TiO_2 nanoparticles with APTES

The diffraction pattern for the pure PAI shown in Fig. 4 (a) demonstrates that the PAI is completely amorphous. Presence of the non-coplanar and twisted moieties into the backbone of polymer decreased the intermolecular forces between the polymer chains and reduced the crystallinity of polymer. Figure 4b displays anatase and rutile phase for pure TiO_2 nanoparticles. The XRD patterns of PAI/TiO_2 nanocomposite (c) indicate characteristic peaks of anatase and rutile of TiO_2 and PAI, respectively, indicating that the morphology of TiO_2 nanoparticles has not been disturbed during the process. The wide weak diffraction peak of PAI still exists, but its intensity decreases. The full-width at half-maximum of the strongest characteristic reflection is used to estimate the average crystallite size by applying the Debye–Scherrer equation. The crystallite size of TiO_2 nanoparticles in PAI is 20 nm, which is consistent with the result determined by statistical analysis of the TEM image, indicating that each individual particle is a single crystal.

TEM analysis was performed for PAI/TiO_2 nanocomposite to identify the distribution of nanoparticles within polymer matrix. Figure 5 shows the TEM image of the nanocomposite 8 wt%. As can be seen, the nanoparticles were well dispersed in the polymer matrix. The nanoparticle sizes of TiO_2 are around 20 nm. The relatively strong interactions between polymer matrix and TiO_2 nanoparticles are responsible for observing the nanoparticles with spherical shapes.

UV–Vis spectra of the PAI/TiO_2 nanocomposites with different inorganic contents are shown in Fig. 6. UV–Vis absorption spectra of nanocomposites showed maximum absorption peaks at 307 and 319 nm as shown in Fig. 6. The UV-shielding ability relates with the scattering and/or absorbance of TiO_2 nanoparticles. The scattering property plays an important role in shielding of UV irradiation. Thus, these nanocomposites have potential to apply as coating to block the UV radiation, especially between 300 and 350 nm. The absorption bands in the UV region are due to the charge transfers of the chromophoric unit of the PAI structure and that of Ti–O–Ti segment.

The thermal properties of pure PAI and PAI hybrid nanocomposites 4 and 10 wt% were studied using STA at a heating rate of 20 °C min^{-1}, under a nitrogen atmosphere. The TGA curves of pure PAI and PAI hybrid nanocomposite 4 wt% are shown in Figs. 7 and 8, respectively. The thermoanalysis data of these samples are summarized in Table 1. These studies show that the nanocomposites are thermally stable up to 400 °C. The 10 % weight loss temperatures of the pure PAI and nanocomposites in nitrogen were recorded in 432, 435 and 461 °C for PAI and PAI hybrid nanocomposites 4 and 10 wt%, respectively. The amount of residue (char yield) of these nanocomposites was more than 53 % at 800 °C. As shown in the Figs. 7 and 8, the thermal stability of nanocomposites is higher than pure PAI that is due to the good compatibility of modified TiO_2 particles with polymer matrix. TiO_2 nanoparticles have high thermal stability due to their larger surface area, so the incorporation of TiO_2 nanoparticles can improve the thermal resistance of nanocomposites.

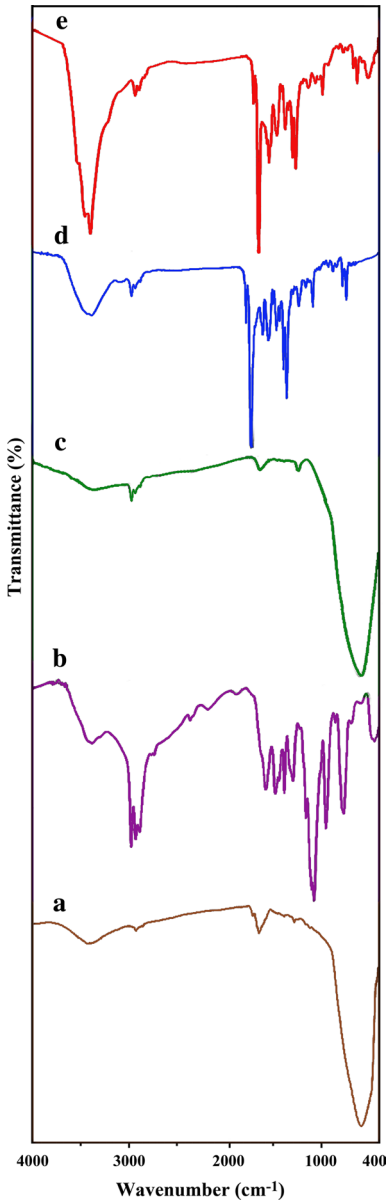

Fig. 2 FT-IR spectra of: *a* as-recevied TiO_2 nanoparticles; *b* pure APTES; *c* APTES-modified TiO_2 nanoparticles; *d* pure PAI; and *e* PAI/TiO_2 4 wt%

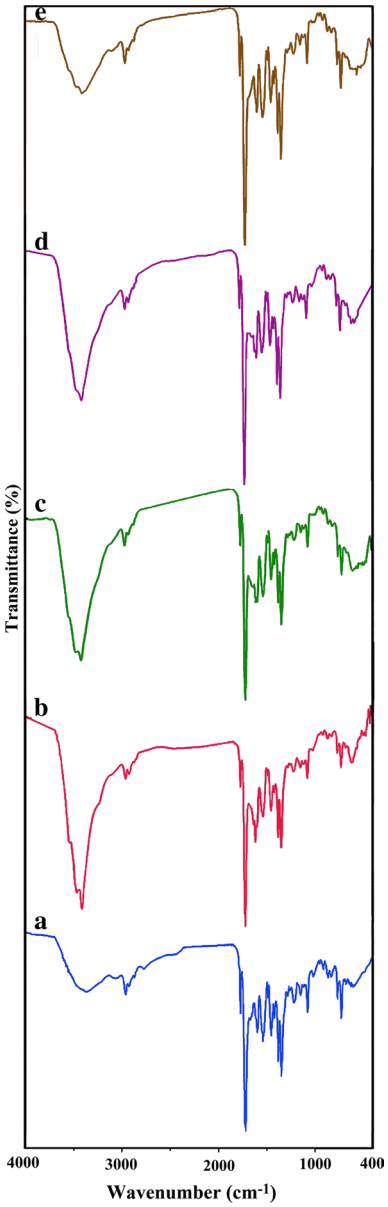

Fig. 3 FT-IR spectra of *a* PAI/TiO_2 (2 wt%); *b* PAI/TiO_2 (4 wt%); *c* PAI/TiO_2 (6 wt%); *d* PAI/TiO_2 (8 wt%); and *e* PAI/TiO_2 (10 wt%)

Char yield can be applied as decisive factor for estimating limiting oxygen index (LOI) of the polymers based on Van Krevelen and Hoftyzer equation (Van Krevelen and Hoftyzer 1976).

$$LOI = 17.5 + 0.4\,CR$$

where CR is the char yield.

The nanocomposites had LOI values calculated derived from their char yield which was higher than 38. On the basis of LOI values, such nanocomposites can be classified as self-extinguishing materials.

Conclusions

Novel optically active amino acid-based PAI/TiO_2 hybrid nanocomposites were successfully prepared under ultrasonic irradiation and characterized by different methods. For prevention of aggregation, the surface of TiO_2 nanoparticles was modified with APTES as a coupling agent. TEM image confirmed nanoscale and homogeneous dispersion of nanoparticles. The TGA and UV–Vis results indicate that the resulting hybrid nanocomposites are thermally stable and could be potentially applied in a coating technology

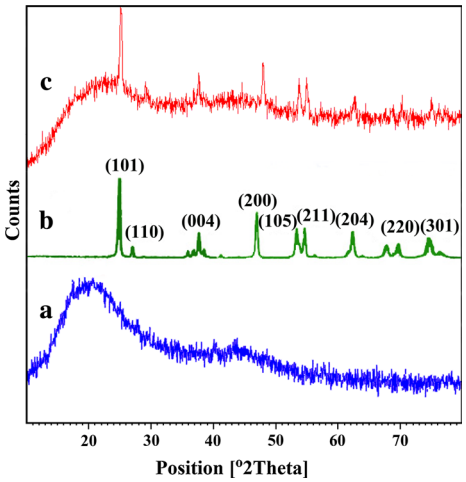

Fig. 4 X-ray diffraction patterns of *a* PAI; *b* pure TiO_2 nanoparticles; and *c* PAI/TiO_2 nanocomposite 8 wt%

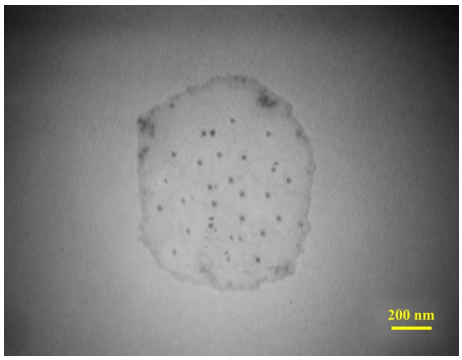

Fig. 5 TEM image of nanocomposite 8 wt%

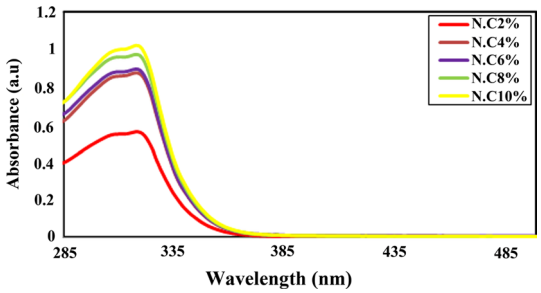

Fig. 6 UV/vis spectra of nanocomposites

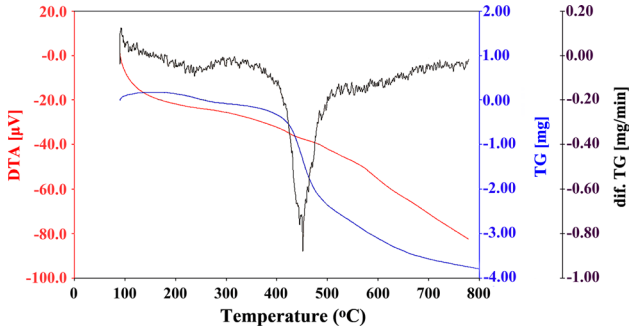

Fig. 7 STA thermogram of pure PAI

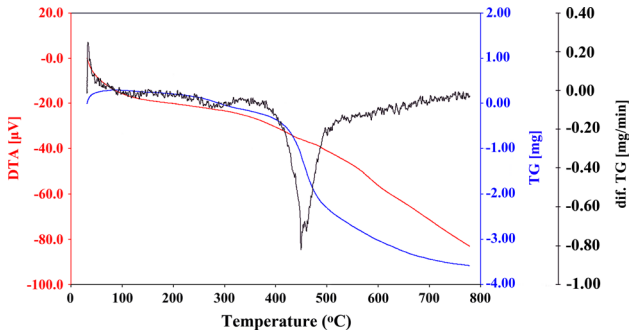

Fig. 8 STA thermogram of nanocomposite 4 wt%

Table 1 Thermal Properties of the pure PAI, PAI/TiO_2 4 wt% and PAI/TiO_2 10 wt%

Sample	Decomposition temperature (°C)		Char yield (%)	LOI
	T_5^a	T_{10}^b		
PAI	404	432	47	36.2
PAI/TiO_2 4 wt%	404	435	53	38.6
PAI/TiO_2 10 wt%	437	461	62	42.3

[a] Temperature at which 5 % weight loss was recorded by TGA at a heating rate of 20 °C/min under nitrogen atmosphere

[b] Temperature at which 10 % weight loss was recorded by TGA at a heating rate of 20 °C/min under nitrogen atmosphere

[c] Percentage weight of material left undecomposed after TGA analysis at maximum temperature 800 °C under nitrogen atmosphere

to shield against UV light, respectively. Since this PAI has amino acid in its polymer architecture, it could be categorized under environmentally benign polymers and could be composted with organic wastes and recycled to enrich the soil. Also, it has the potential to be applied as optically active packing materials in column chromatography for the resolution of racemic mixtures. Polymers that are prepared from naturally occurring building blocks such as amino acids are favorable materials for pharmaceutical and biomedical purposes since their degradation products are nontoxic and can be metabolized correctly by alive tissues. Combining nanosized bioactive materials with biopolymer could generate materials with greater bioactivity and better mechanical properties. Thus, having both natural amino acid and TiO_2 nanoparticles in these novel nanocomposites,

it would be suitable to name them as bionanocomposites macromolecules which may be anticipated to have biodegradability and biocompatibility properties.

Conflict of interest None.

References

Ayala V, Maya EM, Garcia JM, De La Campa JG, Lozano AE, De Abajo J (2005) Synthesis, characterization, and water sorption properties of new aromatic polyamides. J Polym Sci Part A Polym Chem 43:112–121

Baughman TW, Wagener KB (2005) Recent advances in ADMET polymerization, metathesis polymerization. Adv Polym Sci 176:1–42

Derlyukova LE, Anufrieva TA, Grigoreva AV, Vinokurov AA (2012) Oxidizing catalysts supported on nanostructured TiO_2. Inorg Mater 48:914–917

El-Sherbiny S, Morsy F, Samir M, Fouad OA (2014) Synthesis, characterization and application of TiO_2 nanopowders as special paper coating pigment. Appl Nanosci 4:305–313

Frank AJ, Kopidakis N, van de Lagemaat J (2004) Electrons in nanostructured TiO_2 solar cells: transport, recombination and photovoltaic properties. Coordin Chem Rev 248:1165–1179

Haidry AA, Schlosser P, Durina P, Mikula M, Tomasek M, Plecenik T, Roch T, Pidik A, Stefecka M, Noskovic J, Zahoran M, Kus P, Plecenik A (2011) Hydrogen gas sensors based on nanocrystalline TiO_2 thin films. Cent Eur J Phys 9:1351–1356

Hamciuc C, Hamciuc E, Homocianu M, Nicolescu A, Carja ID (2015) Dyes Pigm 114:110–123

Hu K, Kulkarni DD, Choi I, Tsukruk VV (2014) Graphene-polymer nanocomposites for structural and functional applications. Prog Polym Sci 39:1934–1972

Katsarava R (2003) Active polycondensation: from peptide chemistry to amino acid based biodegradable polymers. Macromol Symp 199:419–429

Lim YS, Tan YP, Lim HN, Huang NM, Tan WT (2013) Preparation and characterization of polypyrrole/graphene nanocomposite films and their electrochemical performance. J Polym Res 20:156–165

Liu X, Chen Q, Lv L, Feng X, Meng X (2015) Preparation of transparent PVA/TiO_2 nanocomposite films with enhanced visible-light photocatalytic activity. Catal Commun 58:30–33

Mallakpour S, Rafiee Z (2011) New developments in polymer science and technology using combination of ionic liquids and microwave irradiation. Prog Polym Sci 36:1754–1765

Mallakpour S, Shahmohammadi MH (2005) Synthesis of new optically active poly(amide–imide)s derived from *N*,*N*′-(pyromellitoyl)-bis-S-valine diacid chloride and aromatic diamines under microwave irradiation and classical heating. Iran Polym J 14:473–483

Mallakpour S, Abdolmaleki A, Rostami M (2014) Hybrid S-valine functionalized multi-walled carbon nanotubes/poly(amid-imide) nanocomposites containing trimellitimidobenzene and 4-hydroxyphenyl benzamide moieties: preparation, processing, and thermal properties. J Mater Sci 49:7445–7453

Mallya AN, Kottokkaran R, Ramamurthy PC (2014) Conducting polymer-carbon black nanocomposite sensor for volatile organic compounds and correlating sensor response by molecular dynamics. Sensor Actuat B Chem 201:308–320

Niaounakis M (2013) Biopolymers reuse, recycling, and disposal. Elsevier, New York

Rafiee Z, Golriz L (2014) Synthesis and properties of thermally stable polyimides bearing pendent fluorene moieties. Polym Adv Technol 25:1523–1529

Rafiee Z, Golriz L (2015) Polyimide nanocomposite films containing α-Fe_2O_3 nanoparticles. J Polym Res 22:630–641

Sanda F, Endo T (1999) Syntheses and functions of polymers based on amino acids. Macromol Chem Phys 200:2651–2661

Schneider J, Matsuoka M, Takeuchi M, Zhang J, Horiuchi Y, Anpo M, Bahnemann DW (2014) Understanding TiO_2 photocatalysis: mechanisms and materials. Chem Rev 114:9919–9986

Van Krevelen DW, Hoftyzer PJ (1976) Properties of polymers, 3rd edn. Elsevier, Amsterdam

Wang LK, Chen JP, Hung YT, Shammas NK (eds) (2011) Membrane and desalination technologies series: Handbook of environmental engineering. Springer, pp 13